Demagnetization energy and magnetic permeability tensor of spheroidal magnetic particles dispersed in cubic lattices

H. How and C. Vittoria

Department of Electrical and Computer Engineering, Northeastern University, Boston, Massachusetts 02115

The static demagnetization energies as well as the Polder permeability tensors of uniformly magnetized spheroidal particles arranged periodically in three-dimensional lattices have been calculated. The energy is calculated as a function of aspect ratios, packing densities, and local coordinations: simple-cubic, body-centered-cubic, and face-centered-cubic lattices. The demagnetizing energy is expressed in terms of three demagnetizing factors, N_x, N_y, and N_z. We find that N_x, N_y, and N_z are well behaved for packing densities reaching the percolation limit. The Polder permeability tensor of the composite is derived in terms of these three demagnetizing factors and as a function of the particle's aspect ratio and packing density. The magnetic particles may be assumed to be magnetically saturated or nonsaturated.

I. INTRODUCTION

The study of composite materials has been the subject of considerable interest in recent years because of possible technological applications of these materials.[1] In this paper we are considering microwave applications of composite materials consisting of magnetic particles embedded in a binder matrix. Besides the permittivity of the composite, the magnetic permeability is of crucial importance regarding the usefulness of materials, in general, for microwave applications. The problem of calculating the permittivity of composite materials consisting of fine particles uniformly distributed in a binder material has been considered for over 40 years. For a dilute concentration of particles in a composite, the resultant permittivity is the sum of all the single-particle contributions to the total polarization of the composite. For concentrations beyond approximately 20% volume loading, this approach of calculating permittivity is inaccurate, since the distance between particles decreases to a point in which coupling between particles must be included in any realistic calculation. The multipole method of calculations first introduced by Lord Rayleigh[2] is useful in estimating the contribution due to coupling to the permittivity of heavily loaded composites. Reasonable success has been achieved using this method of calculation to determine the resistivity of composites consisting of metallic particles symmetrically distributed with sc, bcc, and fcc coordinations.[3]

In the calculation of permeability for composites consisting of magnetic particles, the above-reference method[2,3] is applicable if one assumes a single magnetic domain nucleation in each particle. The method becomes impractical or unyielding if, for example, the magnetic domain within a particle is coupled to elastic vibrations and an electric dipole moment. The difficulty arises from the fact that the elastic motion or other motions affects the motion of the dipole moment and, hence, the electromagnetic coupling between particles and vice versa.

We propose a new method or formulation of calculation that may prove to be more general. The interaction between particles is represented in an integration representation introduced earlier by Kaczér and Murtinová.[4] This allows us to represent the coupling between particles in terms of energy terms which are only appropriate to a single particle. The implication here is that all the particles have the same form of energy terms. Hence, long-wavelength excitations are assumed. The advantage of this approach is that the free-energy expression of the particle may contain terms representing purely magnetic interaction between particles as well as self-elastic energy terms, magnetic anisotropy energy terms, etc. The particle-particle interaction energy term is manifested in the so-called demagnetizing factors. The effective permeability of the composite can then be calculated in the usual way[5,6] from the total free-energy—self- and particle-particle energy terms.

In the past, Vorob'yev et al.[7] considered the permeability calculations of a magnetic composite in which the permeability was averaged to be a scalar value, and Abe et al.[8] considered the tensor permeability of a composite consisting of fine magnetic particles. Both of these calculations were carried out under the assumption that the loading of particles in a binder material is dilute and the interaction between the particles is small compared to the self-energy of the particles. In the dilute limit the permeability of the composite is expected to have a linear dependence on the particle volume loading and have small dependence on the particles' shape. The above model is inappropriate to the volume loading of particles in which the particle might ultimately reach a percolation packing limit (particles touching each other).

In this paper we first consider calculations of the demagnetizing field which represents the magnetic interaction between particles arranged in cubic lattices. The demagnetizing fields are calculated as a function of the particle's aspect ratio and concentration. The permeability tensor of the composite is then calculated from

the total energy which includes the demagnetizing, magnetizing, and anisotropy energies. Thus, the total energy is sufficiently general so that it may include particles which are magnetically saturated or nonsaturated. The effect of the particle's axial anisotropy is also incorporated in the calculations.

II. CALCULATIONS

A. Demagnetizing energy

Let the z axis be the revolution axis of the spheroidal particles which are arranged periodically in free space. The case where the binding medium is characterized by the dielectric constant ϵ_1 and magnetic permeability μ_1 can be deduced by replacing ϵ (dielectric constant of the particles), μ (magnetic permeability of the particles), and k (wave number) of the text by ϵ/ϵ_1, μ/μ_1, and $k(\epsilon_1\mu_1)^{1/2}$, respectively, and multiplying all electric fields (including the exciting field) by $(\epsilon_1)^{-1/2}$ and all magnetic fields by $(\mu_1)^{-1/2}$. We only consider here cubic lattices and the conventional unit cell for a bcc structure is shown in Fig. 1. We denote a and b as the semimajor and semiminor axes of the particles, respectively, and all the lengths have been normalized with respect to the length of a unit cell. The analysis below utilizes the formalism developed in Ref. 4 and Gaussian units are used throughout.

Let the magnetization vector $\mathbf{M}(x,y,z)$. The Fourier component of M_α is denoted as $C_{\mathbf{k}}^{(\alpha)}$ with

$$M_\alpha(\mathbf{r}) = \sum_{\mathbf{k}} C_{\mathbf{k}}^{(\alpha)} e^{-i\mathbf{k}\cdot\mathbf{r}} , \tag{1a}$$

$$C_{\mathbf{k}}^{(\alpha)} = \int_{-1/2}^{1/2} dx \int_{-1/2}^{1/2} dy \int_{-1/2}^{1/2} dz\, M_\alpha(\mathbf{r}) e^{i\mathbf{k}\cdot\mathbf{r}} . \tag{1b}$$

Here,

$$\mathbf{k} = 2\pi(p\hat{x} + q\hat{y} + r\hat{z}) \tag{1c}$$

is the wave vector with p,q,r being integers from $-\infty$ to $+\infty$. The magnetostatic potential associated with magnetic charge M_α satisfies the following Poisson equation:

$$\nabla^2 \psi^{(\alpha)} = -4\pi M_\alpha , \tag{2a}$$
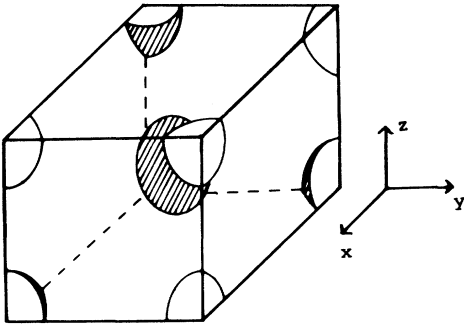
which implies, from Eq. (1a),

FIG. 1. Unit cell for a bcc lattice containing prolate spheroidal particles.

$$\psi^{(\alpha)}(\mathbf{r}) = \sum_{\mathbf{k}}' \frac{4\pi}{k^2} C_{\mathbf{k}}^{(\alpha)} e^{-i\mathbf{k}\cdot\mathbf{r}} , \tag{2b}$$

where $\sum_{\mathbf{k}}'$ denotes the summation over all the vectors of $\mathbf{k}$ except the term $\mathbf{k}=0$. The term $\mathbf{k}=0$ corresponds to the self-energy of the magnetization distribution which appears in a later formulation and is therefore omitted. The demagnetizing field associated with $M^{(\beta)}$ in the α direction is[4]

$$H_\alpha^{(\beta)}(\mathbf{r}) = \frac{\partial^2 \psi^{(\beta)}}{\partial x_\alpha \partial x_\beta}$$

$$= -4\pi \sum_{\mathbf{k}}' \frac{k_\alpha k_\beta}{k^2} C_{\mathbf{k}}^{(\beta)} e^{-i\mathbf{k}\cdot\mathbf{r}} . \tag{3}$$

The demagnetizing energy density is therefore

$$E = \int_{-1/2}^{1/2} dx \int_{-1/2}^{1/2} dy \int_{-1/2}^{1/2} dz\, \mathbf{M}(\mathbf{r})\cdot\mathbf{H}(\mathbf{r})$$

$$= \sum_{\alpha,\beta=1}^{3} E_{\alpha\beta} , \tag{4}$$

where $E_{\alpha\beta}$ is defined by

$$E_{\alpha\beta} = \int_{-1/2}^{1/2} dx \int_{-1/2}^{1/2} dy \int_{-1/2}^{1/2} dz\, M_\alpha(\mathbf{r}) H_\alpha^{(\beta)}(\mathbf{r})$$

$$= 2\pi \sum_{\mathbf{k}}' C_{\mathbf{k}}^{(\alpha)} \cdot C_{\mathbf{k}}^{(\beta)} \cdot \frac{k_\alpha k_\beta}{k^2} . \tag{5}$$

If the magnetization distribution possesses even parity, $\mathbf{M}(\mathbf{r}) = \mathbf{M}(-\mathbf{r})$, it implies $C_{\mathbf{k}}^{(\alpha)} = C_{-\mathbf{k}}^{(\alpha)}$ and so $E_{\alpha\beta} = 0$ if $\alpha \neq \beta$. Therefore, for cubic lattices we have

$$E = \sum_{\alpha=1}^{3} E_{\alpha\alpha} \tag{6a}$$

with

$$E_{\alpha\alpha} = 2\pi \sum_{\mathbf{k}}' \left[C_{\mathbf{k}}^{(\alpha)} \frac{k_\alpha}{k} \right]^2 . \tag{6b}$$

We assume the particles are magnetized uniformly and the magnetization vector $\mathbf{M}(\mathbf{r})$ takes the following form:

$$\mathbf{M}(\mathbf{r}) = \begin{cases} M_{0x}\hat{x} + M_{0y}\hat{y} + M_{0z}\hat{z} , \\ \qquad\qquad \text{for } \mathbf{r} \text{ located within the particles,} \\ 0, \quad \text{otherwise} . \end{cases}$$

We define the volume integral $I_{\mathbf{k}}$ and the form factor $F_{\mathbf{k}}$ as the following:

$$I_{\mathbf{k}} = \underset{\substack{\text{single}\\\text{particle}}}{\int\int\int} d\tau\, e^{i\mathbf{k}\cdot\mathbf{r}} , \tag{7a}$$

$$F_{\mathbf{k}} = \begin{cases} 1, \quad \text{for sc lattice,} \\ [1+(-1)^{p+q+r}], \quad \text{for bcc lattice,} \\ [1+(-1)^{p+1}+(-1)^{q+r}+(-1)^{r+p}] , \\ \qquad\qquad\qquad\qquad \text{for fcc lattice} . \end{cases} \tag{7b}$$

It turns out that

$$C_{\mathbf{k}}^{(\alpha)} = M_{0\alpha} I_{\mathbf{k}} F_{\mathbf{k}} . \tag{8}$$

Denote v as the volume fraction of the particles and n as the number of particles per unit cell ($n = 1$, 2, and 4 for sc, bcc, and fcc structures, respectively). The demagnetizing factor N_α is defined by

$$N_\alpha = \frac{n^2}{v(1-v)} \sum_{\mathbf{k}}' \left| \frac{I_\mathbf{k} F_\mathbf{k} k_\alpha}{k} \right|^2 , \tag{9}$$

and Eqs. (6a) and (6b) can be rewritten as

$$E = \frac{2\pi v(1-v)}{n^2} \sum_{\alpha=1}^{3} N_\alpha M_{0\alpha}^2 . \tag{10}$$

Normalization factors are self-contained in Eq. (9) such that

$$N_x + N_y + N_z = 1 . \tag{11}$$

Equation (11) can be verified utilizing Eq. (9) and notice that the $\mathbf{k} = 0$ term is omitted in the summation.

The remaining work is to calculate $I_\mathbf{k}$. For spherical particles, $a = b$,

$$I_\mathbf{k} = \frac{4\pi}{k^3} \int_0^{ka} \zeta \sin\zeta \, d\zeta , \tag{12}$$

where the equality

$$e^{i\mathbf{k}\cdot\mathbf{r}} = \sum_{l=0}^{\infty} i^l (2l+1) j_l(kr) P_l(\cos\gamma)$$

has been used and only the $l = 0$ term contributes to the volume integral of $I_\mathbf{k}$. Here j_l is the spherical Bessel function of order l [$j_0(\zeta) = (\sin\zeta)/\zeta$], and γ is the angle between $\mathbf{k}$ and $\mathbf{r}$. For spheroidal particles it is derived in the Appendix that

$$I_\mathbf{k} = 4\pi \int_c^a ds \left\{ \left[s^2 + \left[-\frac{k_z^2 s^2 + 1}{Z^2} + \frac{3k_z^2 s^2}{Z^4} \right] c^2 \right] \frac{\sin Z}{Z} \right.$$
$$\left. + \left[\frac{1}{Z^2} - \frac{3k_z^2 s^2}{Z^4} \right] c^2 \cos Z \right\} ,$$

for prolate spheroids , (13a)

$$= 4\pi \int_0^b ds \left\{ \left[s^2 + \left[\frac{k_z^2 s^2 + 1}{X^2} - \frac{3k_z^2 s^2}{X^4} \right] c^2 \right] \frac{\sin X}{X} \right.$$
$$\left. + \left[\frac{-1}{X^2} + \frac{3k_z^2 s^2}{X^4} \right] c^2 \cos X \right\} ,$$

for oblate spheroids , (13b)

where Z and X are defined as

$$Z = [k^2 s^2 - (k_x^2 + k_y^2)c^2]^{1/2} ,$$

$$X = [k^2 s^2 + (k_x^2 + k_y^2)c^2]^{1/2} ,$$

and c is the focal length of the particles defined by

$$c = (a^2 - b^2)^{1/2} .$$

Note that X and Z go to zero if $k_z = 0$, $s = c$, and if $k_x = k_y = 0$, $s = 0$, respectively. However, in these cases the integrands of $I_\mathbf{k}$ take the same limit form, $4\pi s^2$.

Equations (13a) and (13b) reduce to Eq. (12) in the spheric limit, i.e., $a = b$ and $c = 0$.

B. Polder permeability tensor

Let the particles possess a uniaxial magnetic anisotropy along the particles' axial axes and an external field be applied along x axis. We assume that single magnetic domain formation occurs in every particle. The total free-energy density is therefore composed of the Zeeman energy term, the anisotropy energy term, and the demagnetizing energy term as

$$F = -vH_0 M_x + vK(M_x^2 + M_y^2)/M_s^2 + E_N$$
$$= -vH_0 M_s \sin\theta \cos\phi + vK \sin^2\theta$$
$$+ \frac{2\pi v(1-v)}{n^2} M_s^2 (N_x \sin^2\theta \cos^2\phi$$
$$+ N_y \sin^2\theta \sin^2\phi + N_z \cos^2\theta) , \tag{14}$$

where M_s is the saturation magnetization, H_0 the external field strength, and K the anisotropy constant. Here we have ignored the free-energy term arising from the interfacial energy between the particles and the binding matrix. At static equilibrium we have

$$\frac{\partial F}{\partial \theta} = 0 = \frac{\partial F}{\partial \phi} . \tag{15}$$

This implies

$$\phi_0 = 0 , \tag{16a}$$

$$\theta_0 = \begin{cases} \sin^{-1}[H_0/(H_A + H_N)], & \text{for } H_0 < H_A + H_N , \\ \pi/2, & \text{otherwise} . \end{cases} \tag{16b}$$

Here ϕ_0 and θ_0 denote the equilibrium values of ϕ and θ, H_A is the effective anisotropy field associated with the particle's uniaxial magnetic anisotropy, and H_N is the demagnetizing field arising from the magnetostatic interaction of the particles with itself as well as with its surroundings. H_A and H_N are defined as

$$H_A = 2K/M_s , \tag{17a}$$

$$H_N = 4\pi(1-v)(N_x - N_z)M_s/n^2 . \tag{17b}$$

For $H_0 < H_A + H_N$ the magnetization is not aligned along the applied field, and for $H_0 > H_A + H_N$ the magnetization of the particles is saturated and along H_0. Note that, for a composite consisting of oblate particles, it is possible to have $H_A + H_N < 0$. In this case the magnetization aligned in the $\hat{z}$ direction is in a metastable configuration of the magnetization. An infinitesimal application of H_0 will rotate the magnetization into the x axis.

The effective field associated with the free-energy density of Eq. (2) is[19]

$$\mathbf{H}_e = (-1/v)\nabla_\mathbf{M} F , \tag{18}$$

where $\nabla_\mathbf{M} F$ denotes the functional derivative of F with respect to $\mathbf{M}$, i.e.,

$$(\mathbf{H}_e)_x = H_0 - H_A M_x / M_s - 4\pi(1-v)N_x M_x / n^2 , \quad (19a)$$

$$(\mathbf{H}_e)_y = -H_A M_y / M_s - 4\pi(1-v)N_y M_y / n^2 , \quad (19b)$$

$$(\mathbf{H}_e)_z = -4\pi(1-v)N_z M_z / n^2 . \quad (19c)$$

The Landau-Lifshitz equation takes the form

$$\frac{1}{\gamma}\frac{d\mathbf{M}}{dt} = \mathbf{M} \times \mathbf{H} - \frac{\lambda}{\gamma M^2}\mathbf{M} \times (\mathbf{M} \times \mathbf{H}) , \quad (20)$$

where γ and λ denote, respectively, the gyromagnetic ratio and the Landau-Lifshitz damping constant. Let $\mathbf{M}$ and $\mathbf{H}$ be expressed as

$$\mathbf{M} = \mathbf{M}_0 + \mathbf{m} , \quad (21a)$$

$$\mathbf{H} = \mathbf{H}_e + \mathbf{h} , \quad (21b)$$

where $\mathbf{M}_0$ and $\mathbf{H}_e$ denotes static values of the magnetization and field given by

$$\mathbf{M}_0 = M_s \sin\theta_0 \hat{x} + M_s \cos\theta_0 \hat{z} \quad (22)$$

and by Eqs. (19a)–(19c), respectively. Here $\mathbf{m}$ and $\mathbf{h}$ represent small departures of the magnetization and field away from their equilibrium values. Substituting Eqs. (21a) and (21b) into Eq. (20) and keeping only to first order terms in λ, m, and h, one obtains

$$\frac{-i\omega}{\gamma}\mathbf{m} = \mathbf{m} \times \mathbf{H}'_e + \mathbf{M}_0 \times \mathbf{h} , \quad (23)$$

where $\mathbf{H}'_e$ is defined by

$$(\mathbf{H}'_e)_x = H_0 - [H_A + (4\pi/n^2)(1-v)N_x M_s$$
$$+ i\Delta H/2]\sin\theta_0 , \quad (24a)$$

$$(\mathbf{H}'_e)_y = 0 , \quad (24b)$$

$$(\mathbf{H}'_e)_z = -[(1-v)N_z M_s + i\Delta H/2]\cos\theta_0 , \quad (24c)$$

and ΔH is the linewidth defined by

$$\Delta H = 2\lambda\omega / \gamma^2 M_s . \quad (25)$$

The remaining work is to specify $\mathbf{m}$ and $\mathbf{h}$ explicitly for different purposes. To be valid in first order, $\mathbf{m}$ is perpendicular to $\mathbf{M}_0$ and can be written as

$$\mathbf{m} = m_1 \cos\theta_0 \hat{x} + m_2 \hat{y} + m_1 \sin\theta_0 \hat{z} . \quad (26)$$

$\mathbf{h}$ can be distinguished as being composed of two components

$$\mathbf{h} = \mathbf{h}_e + \mathbf{h}_m \quad (27)$$

with $\mathbf{h}_e$ being the applied rf field and $\mathbf{h}_m$ the field associated with $\mathbf{m}$. From Eqs. (19a)–(19c) $\mathbf{h}_m$ can be written as

$$(\mathbf{h}_m)_x = -[H_A/M_s + 4\pi(1-v)N_x/n^2]m_1\cos\theta_0 , \quad (28a)$$

$$(\mathbf{h}_m)_y = -[H_A/M_s + 4\pi(1-v)N_y/n^2]m_2 , \quad (28b)$$

$$(\mathbf{h}_m)_z = 4\pi(1-v)N_z m_1 \sin\theta_0 . \quad (28c)$$

Without an applied rf field, Eq. (23) determines the ferromagnetic resonant frequency of the composite material. In this case, substituting Eqs. (22), (24), and (26)–(28) into Eq. (23) with $\mathbf{h}_e = 0$, one obtains

$$\begin{bmatrix} \Omega & A \\ -B & \Omega \end{bmatrix}\begin{bmatrix} m_1 \\ m_2 \end{bmatrix} = 0 , \quad (29)$$

where

$$\Omega = i\omega/\gamma , \quad (30a)$$

$$A = H_0/\sin\theta_0 - i\Delta H/2 , \quad (30b)$$

$$B = |H_A + H_N - H_0\sin\theta_0| - i\Delta H/2 . \quad (30c)$$

When the particles' magnetization is saturated, i.e., $H_0 > H_A + H_N$, $\theta_0 = 90°$ and Eqs. (30b) and (30c) become

$$A = H_0 - i\Delta H/2 , \quad (31a)$$

$$B = H_0 - H_A - H_N - i\Delta H/2. \quad (31b)$$

Nonsingular solutions of Eq. (20) exist only if $\Omega^2 + AB = 0$, which solves the ferromagnetic resonant frequency, denoted as ω_H. For nonsaturated particles, one obtains

$$\frac{\omega_H}{\gamma} = H_0\cos\theta_0 - \frac{i\Delta H}{2}(\cos\theta_0 + \sec\theta_0)/2 , \quad (32a)$$

and for saturated particles,

$$\frac{\omega_H}{\gamma} = \sqrt{H_0(H_0 - H_A - H_N)}$$
$$- \frac{i\Delta H}{2}\frac{2H_0 - H_A - H_N}{2}\Big/\sqrt{H_0(H_0 - H_A - H_N)} . \quad (32b)$$

Note that the real part of ω_H goes to zero when the particles just reach saturation, and the imaginary part of ω_H, denoting the linewidth at resonance, always has values larger than that of the bulk material composing the magnetic particles.

Magnetic permeability can be determined from Eq. (23) if the external rf field $\mathbf{h}_e$, is nonvanishing. For $\mathbf{h}_e \neq 0$, an additional term of torque, $\mathbf{M}_0 \times \mathbf{h}_e$, appears on the right-hand side of Eq. (23) and, therefore, it is sufficient to consider $\mathbf{h}_e$ of the following form:

$$\mathbf{h}_e = h_1\cos\theta_0\hat{x} + h_2\hat{y} - h_1\sin\theta_0\hat{z} . \quad (33)$$

Equation (29) now becomes

$$\begin{bmatrix} \Omega & A \\ -B & \Omega \end{bmatrix}\begin{bmatrix} m_1 \\ m_2 \end{bmatrix} = M_s\begin{bmatrix} h_2 \\ -h_1 \end{bmatrix} , \quad (34)$$

which can be rewritten as

$$\begin{bmatrix} m_1 \\ m_2 \end{bmatrix} = \frac{M_s}{\Omega^2 + AB}\begin{bmatrix} A & \Omega \\ -\Omega & B \end{bmatrix}\begin{bmatrix} h_1 \\ h_2 \end{bmatrix} . \quad (35)$$

Therefore, in the coordinate system, whose z axis has been rotated a θ_0 degree toward the x axis, i.e., the new z axis is aligned along $\mathbf{M}_0$, the permeability tensor takes the following form:

$$\underline{\mu}' = \begin{bmatrix} \mu_1 & i\kappa & 0 \\ -i\kappa & \mu_2 & 0 \\ 0 & 0 & 1 \end{bmatrix} , \quad (36)$$

where

$$\mu_1 = 1 + 4\pi v M_s A /(\Omega^2 + AB) , \qquad (37a)$$

$$\mu_2 = 1 + 4\pi v M_s B /(\Omega^2 + AB) , \qquad (37b)$$

$$i\kappa = 4\pi v M_s \Omega /(\Omega^2 + AB) . \qquad (37c)$$

Note that $\underline{\mu}'$ is Hermitian if and only if A and B are real, i.e., the particle medium is lossless. When expressed in the original xyz coordinate system, the permeability tensor becomes

$$\underline{\mu} = \begin{bmatrix} \cos\theta_0 & 0 & \sin\theta_0 \\ 0 & 1 & 0 \\ -\sin\theta_0 & 0 & \cos\theta_0 \end{bmatrix} \cdot \underline{\mu}' \cdot \begin{bmatrix} \cos\theta_0 & 0 & -\sin\theta_0 \\ 0 & 1 & 0 \\ \sin\theta_0 & 0 & \cos\theta_0 \end{bmatrix} . \qquad (38)$$

For magnetization-saturated particles, Eq. (38) can be most conveniently written as

$$\underline{\mu} = \begin{bmatrix} 1 & 0 & 0 \\ 0 & \mu_2 & i\kappa \\ 0 & -i\kappa & \mu_1 \end{bmatrix} . \qquad (39)$$

III. RESULTS

A. Demagnetizing energy

To obtain N_x, N_y, and N_z numerically, we notice the following two things. For large k values the integrands defining I_k in Eqs. (13a) and (13b) oscillate rapidly. If integers p, q, and r are taken from $-N$ to $+N$, there shall be at least N grid points in evaluating integrals which appeared in Eqs. (13a) and (13b) in order not to create significant error. The second point is that the summation over $\mathbf{k}$ in Eq. (9) converges very slowly. Convergence

within 90% was achieved when N was taken to be 100, i.e., when 8 000 000 Fourier components have been taken into account. However, we notice that the convergence is inversely proportional to N, and, when the sums have been extrapolated by $N = 50$ and 100, the demagnetizing factors N_x, N_y, and N_z can be evaluated with errors less than a few parts in one thousand. Errors associated with N_x, N_y, and N_z can be estimated by comparing their sum to unity, Eq. (11).

Figures 2–4 show the dependences of N_x, N_y, and N_z on the aspect ratio $A = b/a$ for the cases of sc, bcc, and fcc, respectively. In these plots, a was fixed to 0.3 (in units of the length of the unit cell) and b was taken from 0 to 0.3. The left-hand sides of these graphs are for the prolate cases (increasing A for the horizontal coordinate), while the right-hand sides are for the oblate cases (decreasing A for the horizontal coordinate). The central lines separating the two sides represent the sphere cases $a = b = 0.3$. For $b = 0$ this corresponds to $N_x = N_y = 0.5$, $N_z = 0$, for the prolate case (thin rod), and $N_x = N_y = 0$, $N_z = 1$, for the oblate case (flat disc). For $a = b$ the demagnetizing factors are all equal to $\frac{1}{3}$ as we expect for the sphere case. The above results are the same as if the particles were isolated from each other. Actually, for an isolated spheroid,[10] prolate and oblate, respectively,

$$N_z = \begin{cases} (1-e^2)(\tanh^{-1}e - e)/e^3 , & (40a) \\ (1+e^2)(e - \tan^{-1}e)/e^3 , & (40b) \end{cases}$$

and $N_x = N_y = (1 - N_z)/2$, where e is the eccentricity of the particle defined as c/a and c/b for a prolate and an oblate, respectively. For the sc and bcc structures, Figs. 2 and 3, the demagnetizing factors presume values which are almost indistinguishable from those derived for an isolated particle, Eqs. (14a), and (14b). Only for the fcc structure do the demagnetizing factors predict apprecia-
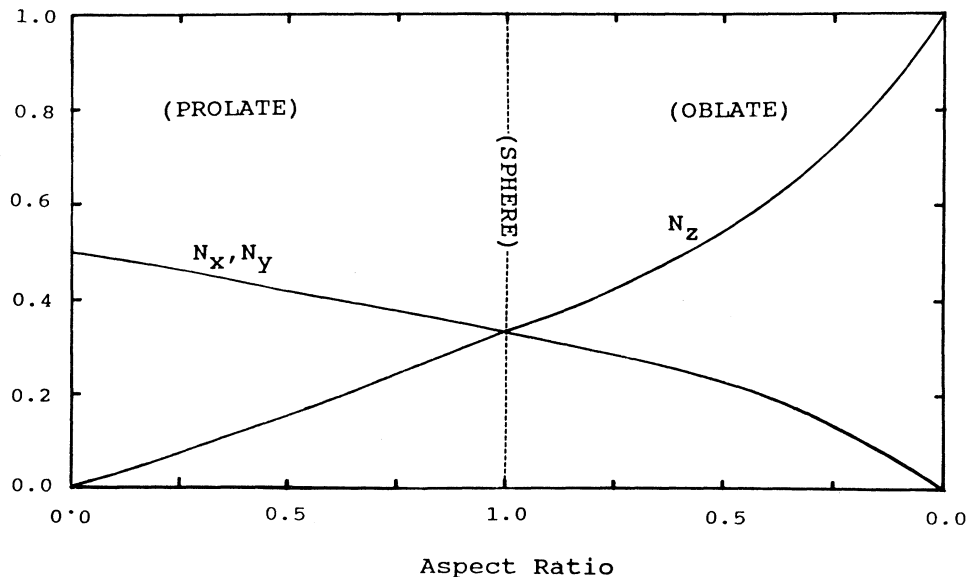

FIG. 2. Demagnetizing factors as functions of the aspect ratio: sc structure. $(a = 0.3, 0 \le b \le a)$.
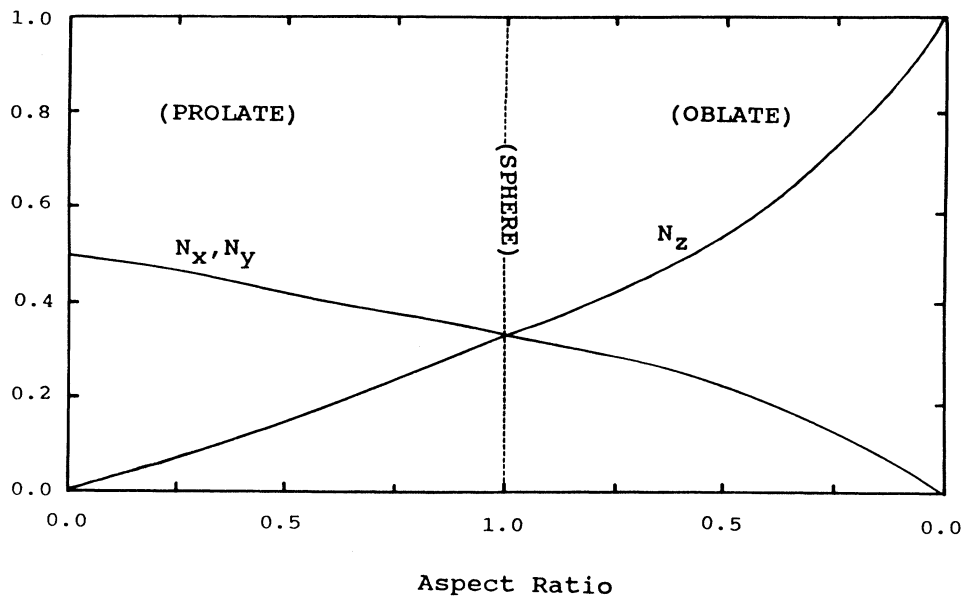
FIG. 3. Demagnetizing factors as functions of the aspect ratio: bcc structure. ($a = 0.3, 0 \leq b \leq a$).

ble departure away from the isolated case. The reason for this is that for the fcc structure with $a = 0.3$ the packing density of the particles is closer to the packing limit, while that of the sc and bcc structures with $a = 0.3$ can still be treated as in the dilute approximation. This point will be discussed further below. However, the demagnetizing energy densities associated with Figs. 2–4 are very different as predicted by Eq. (10).

Figures 5 and 6 show the dependence of N_x, N_y, and N_z on the packing density of the particles in the sc, bcc,

and fcc structures for the cases of prolate and oblate, respectively. The aspect ratio for these plots is chosen to be 0.5 and the horizontal axes are taken to be a. For small a's the curves go to dilute limits which have, from Eqs. (14a) and (14b), the following values: $N_x = N_y = 0.41$, $N_z = 0.17$ for the prolate case, and $N_x = N_y = 0.24$, $N_z = 0.52$ for the oblate case. In the dilute situations where a is small, the demagnetizing factors are almost independent of the particle concentration and have very little dependence on the types of lattice structures, as we
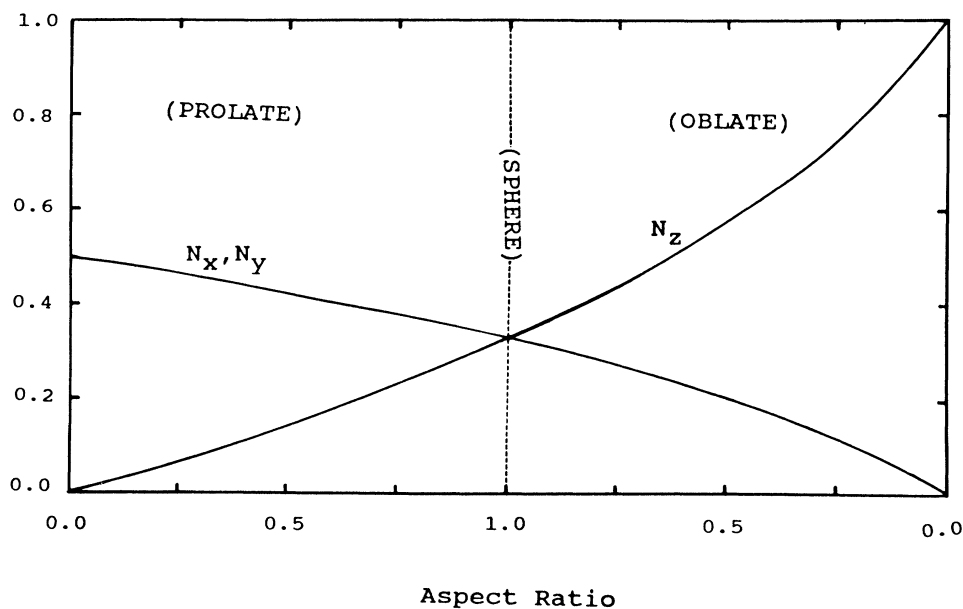
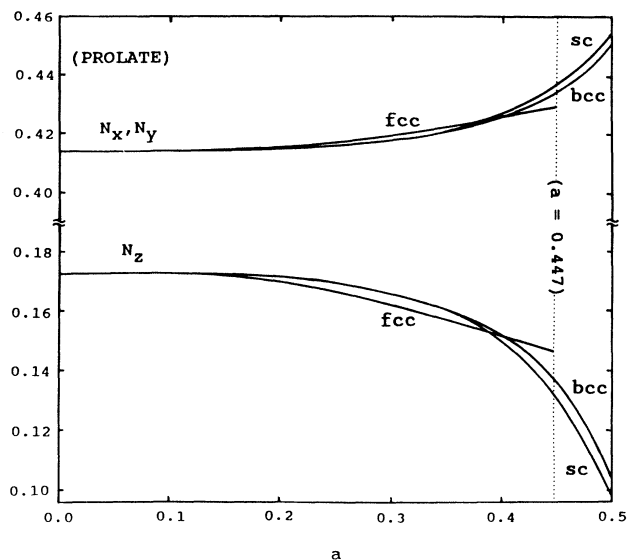FIG. 4. Demagnetizing factors as functions of the aspect ratio: fcc structure. ($a = 0.3, 0 \leq b \leq a$).

FIG. 5. Demagnetizing factors as functions of a for a fixed aspect ratio ($b = a/2$): Prolate case.

might expect. When a increases, the curves gradually depart from their dilute values until the packing limits are finally reached. For the prolate cases the packing limits are 0.5, 0.5, and 0.447 ($=1/\sqrt{5}$), and for the oblate cases 0.5, 0.5, and 0.354 ($=\sqrt{2}/4$) for the sc bcc, and fcc structures, respectively. When the particles' packing limit is approached, the demagnetizing factor closest to the direction parallel to the direction of particles in contact will decrease, as we might expect from the fact that a

long "thread" of magnetic particles have very small demagnetizing factor along its longitudinal direction. However, when the packing limit is reached, there is no catastrophic changes in the values of N_x, N_y, and N_z. This result differs from the situation found in the dielectric-metallic transition in which the metal particles start to touch each other in a dielectric binder.[3] When the packing limit is passed over, Eq. (9) still provides values for N_x, N_y, and N_z, except that in this situation the sum of these physical factors will gradually depart from unity.

B. Polder permeability tensor

In the following calculations we take $4\pi M_s \approx H_A \approx 3000$ G and $\Delta H \approx 100$ Oe (at 9 GHz), which correspond to substantial hexagonal barium ferrite particles. The external field H_0 is normalized with respect to $4\pi M_s$ and angular frequency ω with respect to $4\pi \gamma M_s$. The data for particles in the simple-cubic lattice are calculated explicitly, whereas data concerning bcc and fcc lattices can be deduced in a similar way. Actually, not much difference is found for the functional behavior of the permeability for different particle coordinates in cubic lattices and it will be enough to show the permeability here only for the simple-cubic coordination.

Figure 7 shows, according to Eqs. (32a) and (32b), the resonant frequency as a function of the particle aspect ratio $A = b/a$, where a is chosen to be 0.3 (in units of the length of the lattice unit cell). Two values of the external field have been considered: $H_0 = 0.5$ and 2. The left-hand side of the figure is for the prolate case (increasing A for the horizontal coordinate), the right-hand side is for the oblate case (decreasing A for the horizontal coordinate), and the central line separating the two sides
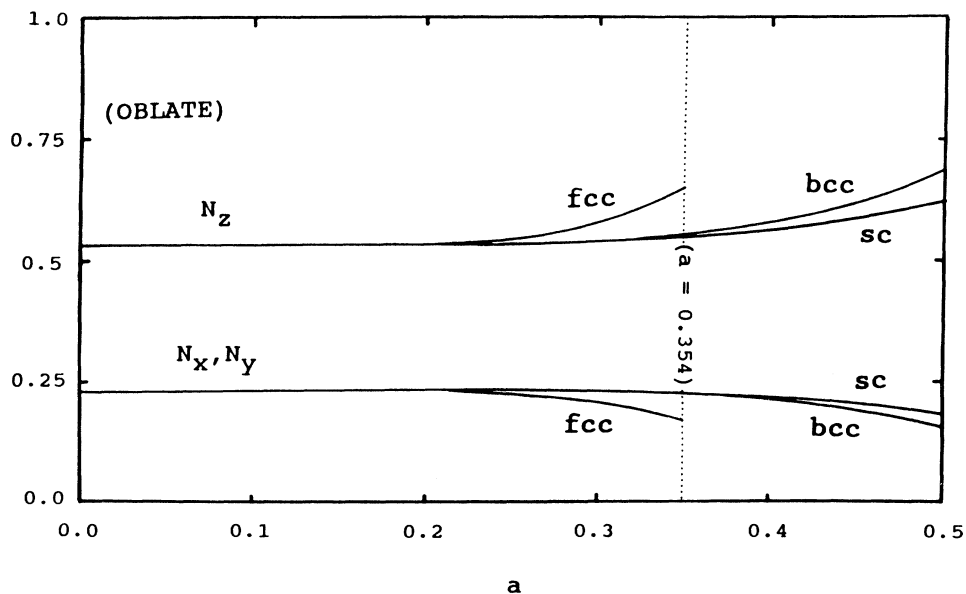

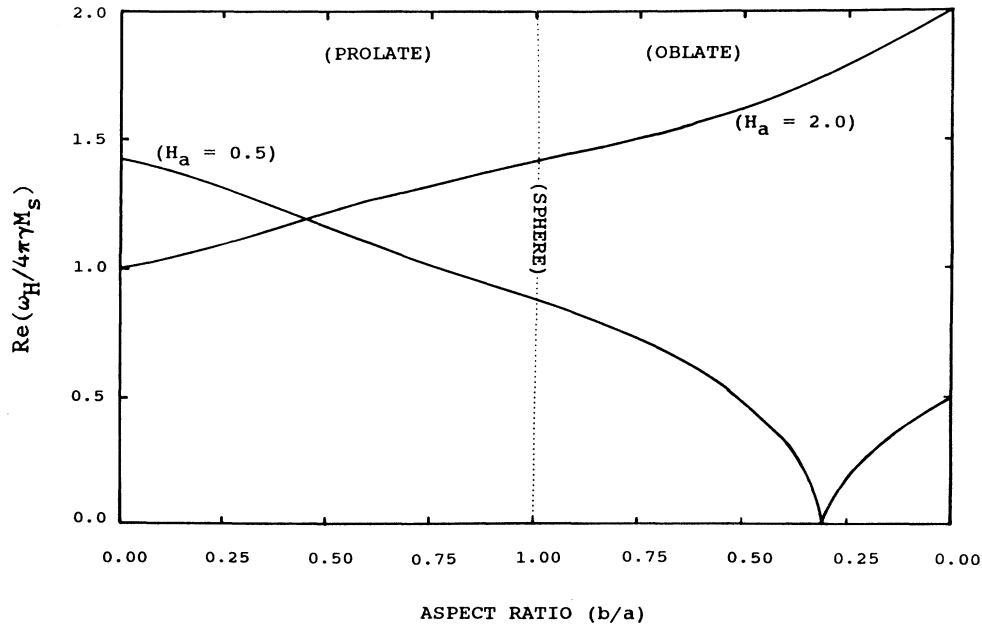FIG. 6. Demagnetizing factors as functions of a for fixed aspect ratio ($b = a/2$): oblate case.

FIG. 7. Resonant frequency as a function of the aspect ratio (b/a) of particles in a simple-cubic lattice: $a = 0.3$, $H_0 = 0.5$, 2.

represents the sphere case $a = b = 0.3$. For $H_0 = 2$ the particles are saturated for all the values of the aspect ratio and the resonant frequency dictates a smooth function over A. For $H_0 = 0.5$ the particle's magnetization is nonsaturated for prolates. It can be saturated for disklike oblates as discussed previously following Eqs. (17a) and (17b). It is shown in Fig. 7 that a cusp ($A = 0.305$) exists in the resonant frequency curve corresponding to $H_0 = 0.5$, which separates the curve in two parts: nonsaturated (left) and saturated (right).

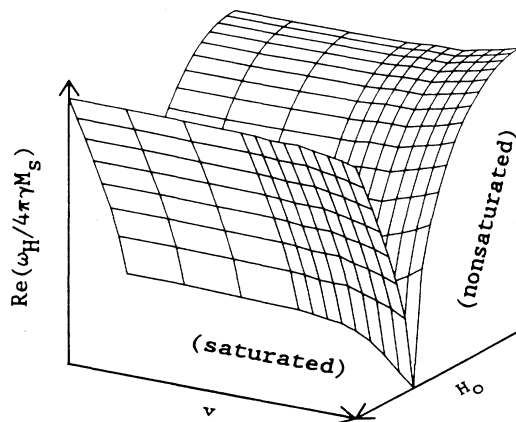Figure 8 shows a three-dimensional plot of the resonant frequency as function of the particle volume fraction

FIG. 8. Resonant frequency as a function of the particle volume fraction v, external field H_0 for prolates ($b = a/2$) with a simple-cubic coordination.

v and the external field H_0. The particles are prolates with $b = a/2$. In this plot v is taken from 0 to 0.13 (maximum particle loading in this case), H_0 from 0 to 2, and the vertical axis, the resonant frequency, from 0 to 1.5. For small H_0 values the particle magnetization is nonsaturated, and in this region the resonant frequency decreases with the increase of H_0. When H_0 goes beyond a certain value, the particle magnetization becomes saturated and the resonant frequency in this region increases with the increase of H_0. The profile of the resonant frequency therefore shows a two-dimensional cusplike surface whose acute end points are located in the horizontal a-H_0 plane. The locus of these end points is shown in Fig. 9. From Figs. 8 and 9 it is seen that the resonant frequency has very little dependence on a if a is small. This situation corresponds to the dilute loading of the particles.

Figures 10 and 11 show, according to Eq. (37a), the real and imaginary parts of μ_1 as functions of the particle volume fraction v and frequency $\omega/4\pi\gamma M_s$, respectively. The particles are prolates with $b = a/2$, and the external field H_0 is chosen to be 0.5. In these plots v is taken from 0 to 0.13 (maximum particle loading in this case), and $\omega/4\pi\gamma M_s$ from 0 to 2. From these figures it is seen that resonance is most pronounced when the particle loading is high. The largest amplitude of resonance occurs at $a = 0.5$, where the peak values of μ_1(real) are 3.3 and -1.12 and the peak of μ_1(imaginary) is 6.93. Away from the resonance μ_1(real) = 1 and μ_1(imaginary) = 0. Plots for μ_2 and κ can also be obtained from Eqs. (37b) and (37c). However, they would show almost identical appearances as for μ_1 in Figs. 10 and 11 and are therefore omitted. We mention here only that the maximum peak values (at $a = 0.5$) are 4.46 and -0.33 for μ_2(real), 6.71
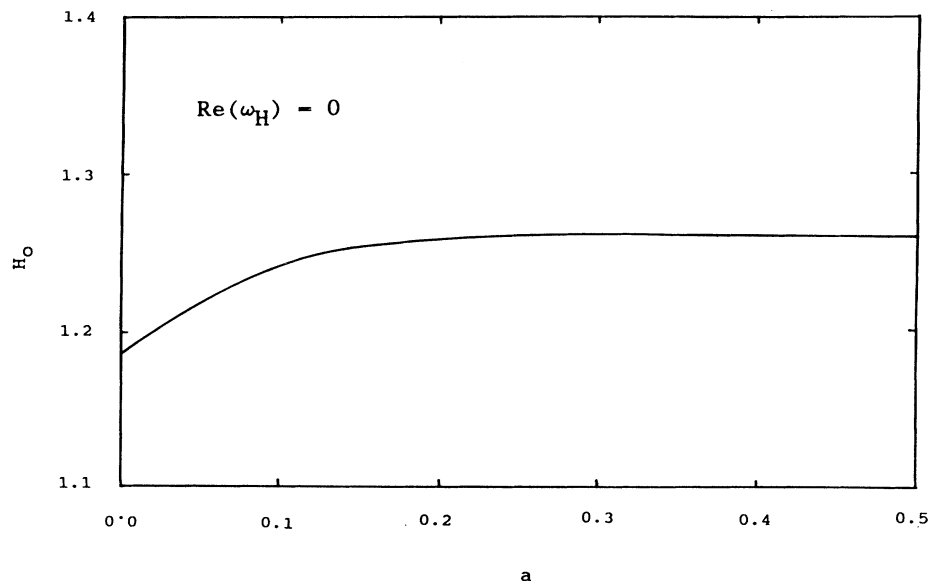
FIG. 9. Saturating field of Fig. 8.

for μ_2(imaginary), 2.21 and -2.09 for κ(real), and 6.42 for κ(imaginary). The common feature of μ_1, μ_2, and κ is that they have very little dependence on a when a is small, again, the situation of dilute particle loading.

IV. CONCLUSIONS

We have calculated the demagnetizing factors associated with magnetic spheroidal particles arranged in cubic lattices. For a dilute concentration of particles, the demagnetizing factors do not vary with the concentration and are independent of the type of lattice structure. When the particle concentration increases further and approaches the percolation limit, the demagnetizing factor, associated with the direction in which the particles are touching, decreases. There is no abrupt change in the demagnetizing factors for the case when the particle density reaches the percolation limit.

The total free energy of the particle contains the demagnetizing energy terms which represent the self-demagnetizing energy and magnetostatic energy coupling from other particles. Although the free energy is purely magnetic, elastic and other energy terms may be added to the total energy of the particle.

Based upon the above free energy, the permeability tensor of the spheroidal magnetic particles dispersed in the same cubic lattices was calculated. The dependence of ω_H, μ_1, μ_2, and κ on the particles' dimension and aspect ratio have been formulated without assuming the dilute particle-loading approximation. We found that the ferromagnetic resonant (FMR) frequency and the per-
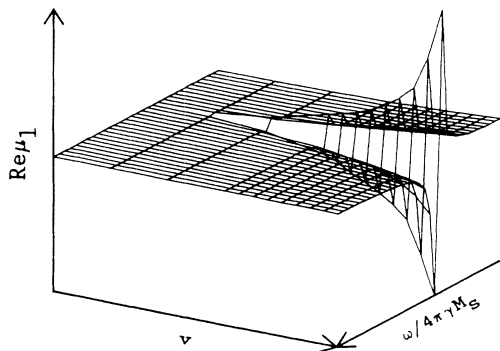

FIG. 10. Real part of μ_1 as a function of the particle volume fraction v and frequency $\omega/4\pi\gamma M_s$, for prolates ($b = a/2$) with a simple-cubic coordination.
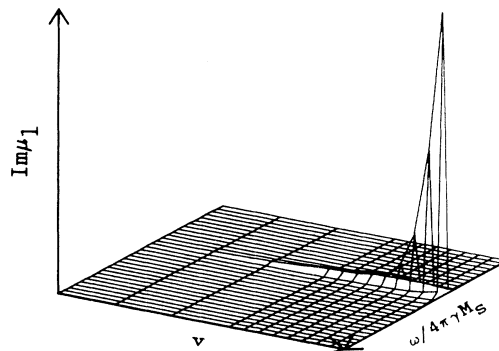

FIG. 11. Imaginary part of μ_1 as a function of the particle volume fraction v and frequency $\omega/4\pi\gamma M_s$ for prolates ($b = a/2$) with a simple-cubic coordination.

meabilities show significant variations only when the particle volume loading is high. No anomalous behavior is found for the permeability even at the percolation limit.

ACKNOWLEDGMENTS

APPENDIX

The prolate spheroidal coordinate (u,v,ϕ) is defined as

$$x = c\ \sinh u\ \sin v\ \cos\phi \ ,$$

$$y = c\ \sinh u\ \sin v\ \sin\phi \ ,$$

$$z = c\ \cosh u\ \cos v \ ,$$

and the volume element is

$$d\tau = dx\ dy\ dz$$

$$= c^3(\sinh^2 u + \sin^2 v)\sinh u\ \sin v\ du\ dv\ d\phi.$$

Consider a single spheroidal particle where the coordinate origin locates at the particle center. The particle surface is bounded by

$$u = u_0 = \cosh^{-1}(a/c) \ .$$

Let the wave vector $\mathbf{k}$ have the spherical coordinate (k,θ_0,ϕ_0). This implies

$$\mathbf{k}\cdot\mathbf{r} = k(x\ \sin\theta_0\cos\phi_0 + y\ \sin\theta_0\sin\gamma_0 + z\ \cos\theta_0)$$

$$= ck[\cosh u\ \cos v\ \cos\theta_0 + \sinh u\ \sin v\ \sin\theta_0\cos(\phi-\phi_0)] \ .$$

Therefore,

$$I_\mathbf{k} = \int\int\int_{\substack{\text{single}\\\text{particle}}} d\tau\, e^{-i\mathbf{k}\cdot\mathbf{r}}$$

$$= c^3\int_0^{u_0} du \int_0^\pi dv(\sinh^2 u + \sin^2 v)\sinh u\ \sin v\ \exp(ick\ \cosh u\ \cos v\ \cos\theta_0)I_1 \ ,$$

where integral I_1 is defined by

$$I_1 = \int_0^{2\pi} d\phi\exp[ick\ \sinh u\ \sin v\ \sin\theta_0\cos(\phi-\phi_0)]$$

$$= 2\pi J_0(ck\ \sinh u\ \sin v\ \sin\theta_0)$$

and J_0 is the Bessel function of order zero defined by

$$J_0(t) = \frac{1}{2\pi}\int_0^{2\pi} d\eta\, e^{it\cos\eta} \ .$$

Therefore, $I_\mathbf{k}$ can be rewritten as

$$I_\mathbf{k} = 2\pi c^3\int_0^{u_0} du(\sinh u)I_2$$

with I_2 defined by

$$I_2 = \int_{-1}^1 d\eta(\cosh^2 u - \eta^2)\exp(ick\ \cos\theta_0\cosh u\ \eta)J_0[ck\ \sin\theta_0\sinh u(1-\eta^2)^{1/2}]$$

$$= 2\int_0^1 d\eta(\cosh^2 u - \eta^2)\cos(\alpha\eta)J_0[\beta(1-\eta^2)^{1/2}] \ .$$

Here, variables α, β, and η are defined by, respectively,

$$\alpha = ck\ \cos\theta_0\cosh u \ ,$$

$$\beta = ck\ \sin\theta_0\sinh u \ ,$$

$$\eta = \cos v \ .$$

After using the following equality,[11] as well as its second derivative,

$$\int_0^1 d\eta\cos(\alpha\eta)J_0[\beta(1-\eta^2)^{1/2}] = \frac{\sin(\alpha^2+\beta^2)^{1/2}}{(\alpha^2+\beta^2)^{1/2}} \ ,$$

one obtains

$$I_\mathbf{k} = 4\pi c^3\int_1^{a/c} d\xi\left[\left[\xi^2 - \frac{c^2k^2\cos^2\theta_0 + 1}{c^2k^2(\xi^2-\sin^2\theta_0)} + \frac{3\cos^2\theta_0\xi^2}{c^2k^2(\xi^2-\sin^2\theta_0)^2}\right]\right.$$

$$\left.\times\frac{\sin[ck(\xi^2-\sin^2\theta_0)^{1/2}]}{ck(\xi^2-\sin^2\theta_0)^{1/2}} + \left[\frac{1}{c^2k^2(\xi^2-\sin^2\theta_0)} - \frac{3\cos^2\theta_0\xi^2}{c^kk^2(\xi^2-\sin^2\theta_0)^2}\right]\cos[ck(\xi^2-\sin^2\theta_0)]^{1/2}\right] \ ,$$

where ξ is defined by

$\xi = \cosh u$.

Now, changing the variable from ξ to s defined by

$s = c\xi$

and noticing that

$$k^2 \sin^2\theta_0 = k_x^2 + k_y^2 \ ,$$

$$k^2 \cos^2\theta_0 = k_z^2 \ ,$$

one obtains Eq. (13a). Equation (13b) can be obtained from Eq. (13a) if c is changed to $-ic$ and the integration limits of s are changed from "c to a" to "0 to b."

---

[1]*Electrical Transport and Optical Properties of Inhomogeneous Media (Ohio State University, 1977)*, Proceedings of the First Conference on the Electrical Transport and Optical Properties of Inhomogeneous Media, AIP Conf. Proc. No. 40, edited by J. C. Garland and D. B. Tanner (AIP, New York, 1978).

[2]J. W. S. Rayleigh, Philos. Mag. **34**, 481 (1982).

[3]W. T. Doyle, J. Appl. Phys. **49**, 795 (1977).

[4]J. Kaczér and L. Murtinová, Phys. Status Solidi A **23**, 79 (1974).

[5]J. O. Artman and S. H. Charap, J. Appl. Phys. **49**, 1587 (1977).

[6]C. Vittoria and F. J. Rachford, J. Appl. Phys. **53**, 8952 (1982).

[7]A. F. Vorob'yev, D. I. Mirovitskiy, V. I. Ponomarenko, and Y. V. Pugachev, Radiotekhnika **3**, 65 (1987).

[8]Masanori Abe and Manabu Gomi, Jpn. J. Appl. Phys. **23**, 1580 (1984).

[9]C. Vittoria and G. C. Bailey, Phys. Rev. B **7**, 2112 (1973).

[10]L. D. Landau and E. M. Lifshitz, *Electrodynamics of Continuous Media* (Pergamon, New York, 1982), p. 25.

[11]J. S. Gradshteyn and I. M. Ryzhik, *Tables of Integrals, Series, and Products* (Academic, New York, 1980), p. 737.